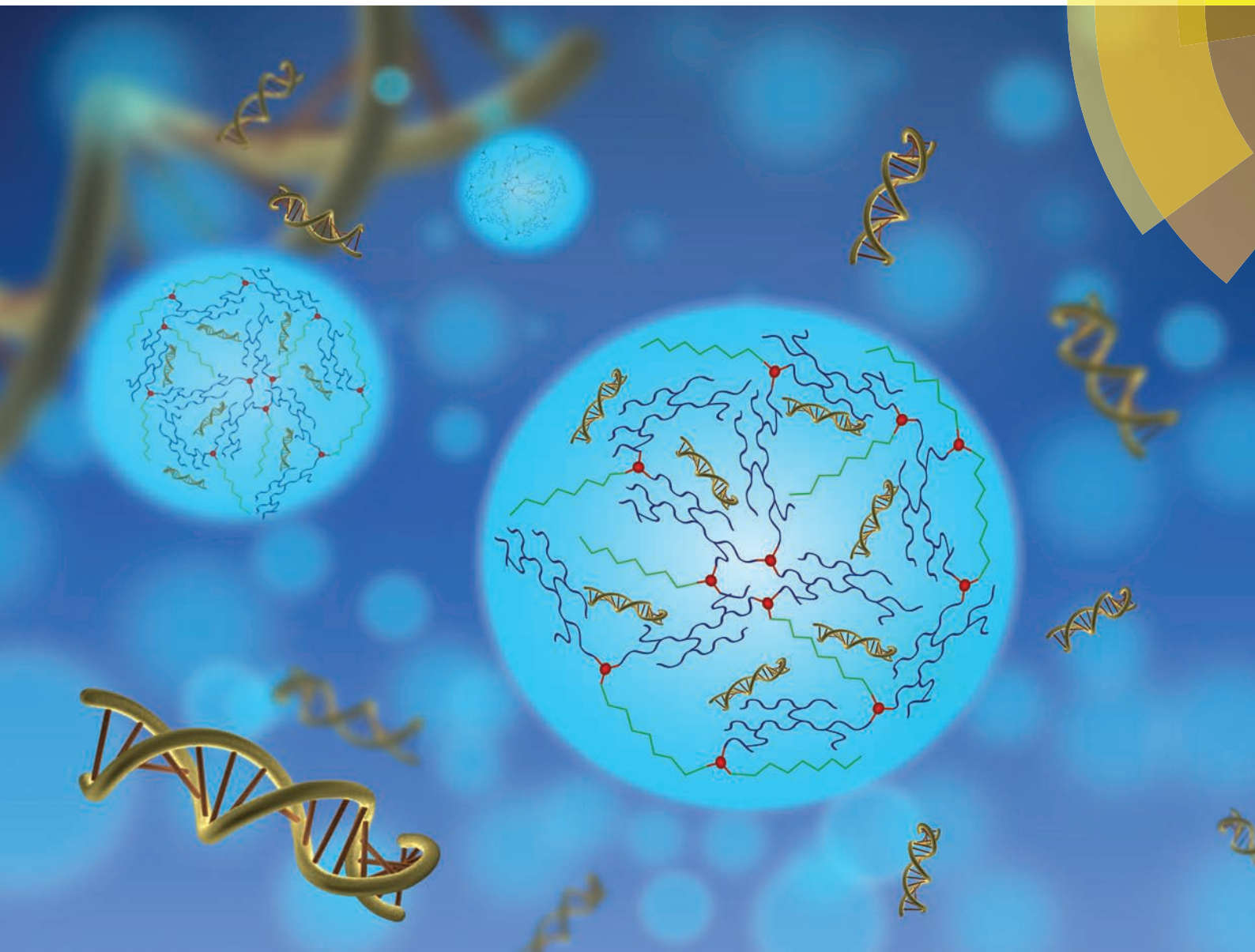


Organic & Biomolecular Chemistry

www.rsc.org/obc



ISSN 1477-0520



PAPER

Mihail Barboiu *et al.*

Dynamic constitutional frameworks (DCFs) as nanovectors for cellular delivery of DNA



Cite this: *Org. Biomol. Chem.*, 2015, **13**, 9005

Dynamic constitutional frameworks (DCFs) as nanovectors for cellular delivery of DNA†

Ioana-Andreea Turin-Moleavin,^a Florica Doroftei,^a Adina Coroaba,^a Dragos Peptanariu,^a Mariana Pinteala,^a Adrian Salic^b and Mihail Barboiu^{*a,c}

We introduce Dynamic Constitutional Frameworks (DCFs), macromolecular structures that efficiently bind and transfect double stranded DNA. DCFs are easily synthesizable adaptive 3D networks consisting of core connection centres reversibly linked *via* labile imine bonds both to linear polyethyleneglycol (PEG, ~1500 Da) and to branched polyethyleneimine (bPEI, ~800 Da). DCFs bind linear and plasmid DNA, forming particulate polyplexes of 40–200 nm in diameter. The polyplexes are stable during gel electrophoresis, well tolerated by cells in culture, and exhibit significant transfection activity. We show that an optimal balance of PEG and bPEI components is important for building DCFs that are non-toxic and exhibit good cellular transfection activity. Our study demonstrates the versatility and effectiveness of DCFs as promising new vectors for DNA delivery.

Received 27th June 2015,
Accepted 8th July 2015

DOI: 10.1039/c5ob01315a

www.rsc.org/obc

Introduction

Gene therapy promises to prevent, treat or cure disease by transferring with minimal side effects, therapeutic genetic material to specific cells or tissues, with the aid of either viral or non-viral vectors.^{1,2} Despite their lower transfection efficiency compared to viral vectors, non-viral gene delivery systems have attracted a lot of attention³ due to their unique advantages such as the ability to deliver single genes and lack of infectivity. Convergent strategies have been used for the design of multivalent molecular, supramolecular and nanometric non-viral vectors⁴ mimicking natural delivery functions: membrane penetration, optimal DNA binding and packing, capacity for endosomal escape or nuclear localization, low cytotoxicity and anti-opsonisation functions.⁵ However, due to the enormous variability of both DNA targets and nature of the transfected cells, rational design has been limited to the introduction of a reduced number of components and had to be accomplished by combinatorial approaches. In this context, the Dynamic Combinatorial Strategy proposed by Matile *et al.*⁶ is one of the most attractive methods for rapid screening, allowing access to active systems from large and complex

libraries. By virtue of reversible covalent exchanges between the hydrophilic heads and hydrophobic tails, the fittest *Dynamic molecular transfectors* can adapt simultaneously to the DNA and the cell membrane barrier.

As for the design approaches, the dynamic constitutional strategy alternative may embody the flow of structural information from molecular to *Dynamic adaptive nanotransfectors*.⁷ This concerns the use of linear Dynamic Polymers (Dynamers)^{8,9} or of cross-linked Dynamic Constitutional Frameworks (DCFs).^{7,10} These structures are composed of specific components and connector centres, linked together by labile, reversible covalent bonds. Importantly, they undergo exchange, incorporation/decorporation of their subunits, synergistically interacting and adapting the overall nanostructure in the presence of DNA and bilayered membrane components. This might play an important role in the ability to finely mutate and adaptively implement reversible rearrangements of the components toward a high level of correlativity of their hypersurfaces in interaction with the DNA and the cell membrane barrier. Thus, this strategy leaves the liberty to DNA systems to self-select and self-generate the carrier best adapted for its own transfection.

We have recently shown that linear PEG macromonomers, trialdehyde core connectors and positively charged guanidinium heads can be used to generate DCFs for DNA recognition.⁷ The simplicity and robustness of the synthetic strategy allow rapid screening of conditions for generating systems with optimal DNA presenting/cell membrane synergistic affinities. Among potential components for the DNA recognition/transfection offered by the available toolbox, large libraries of active compounds may be used for these purposes.

^aAdaptative Supramolecular Nanosystems Group, Institut Européen des Membranes, ENSCM/UMI/UMR-CNRS 5635, Pl. Eugène Bataillon, CC 047, 34095 Montpellier, Cedex 5, France. E-mail: mihail-dumitru.barboiu@univ-montp2.fr

^bDepartment of Cell Biology, Harvard Medical School, 240 Longwood Avenue, Boston, MA 02115, USA

^c“Petru Poni” Institute of Macromolecular Chemistry of Romanian Academy – 41A, Aleea Gr. Ghica Voda, Iasi, Romania

†Electronic supplementary information (ESI) available. See DOI: 10.1039/c5ob01315a

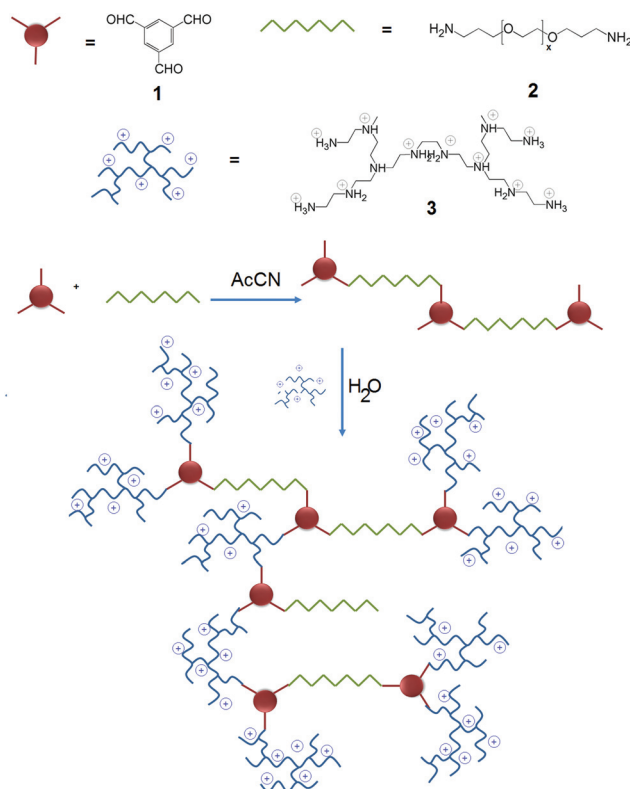
Since its first use as a gene delivery system,³ PEI has been one of the most studied synthetic cationic DNA vectors, and the branched PEI of high molecular weight is considered to be one of the most efficient gene carriers for plasmid DNA, oligonucleotides and small interfering RNAs (siRNAs).² The high transfection efficiency for PEI/DNA polyplexes is attributed to the unique capacity of PEI to buffer endosomes.^{1,11} However, the use of PEI *in vivo* and *in vitro* gene delivery is limited because of its low colloidal stability and its considerable cytotoxicity.² To enhance stability and biocompatibility of PEI polyplexes, they can be combined with PEG; however, PEGs shield the positive charges of PEI, which often has the undesired effect of decreasing transfection efficiency.^{2,12}

Results and discussion

In this study, 1,3,5-benzenetri-aldehyde connectors **1**, poly-(ethylene glycol)-bis(3-aminopropyl) terminated PEG **2** ($M_n \sim 1500 \text{ g mol}^{-1}$), and branched PEI **3** (bPEI, 800 Da) building blocks were used to conceive DCFs for DNA recognition and binding. Treatment of **1** with **2** in different molar ratios (**1** : **2** = 1 : 1, 3 : 2) in acetonitrile (r.t., 72 h) afforded mixtures of linear and cross-linked non-charged frameworks **A1–5** (Table S1, ESI†) assembled *via* reversible amino-carbonyl/imine chemistry (Scheme 1). Then **A1–5** were reacted with bPEI **3** building blocks in water at varying molar ratios to generate the positively charged DCF vectors (Tables S2–S6, ESI†).

NMR experiments

¹H-NMR spectral analysis agrees with the formation of a mixture of imine/aldehyde decorated **A1–5**. The 1 : 1 and 3 : 2 mixtures are reminiscent with the formation of mostly linear polymers, with $M_n \sim 15\,000\text{--}18\,000 \text{ g mol}^{-1}$, as previously observed.⁷ Increasing the amount of **1**, more complex cross-linked frameworks are formed (Fig. S1–S5, ESI†). Interestingly, the ¹H-NMR spectra of DCF mixtures recorded in CD₃CN and D₂O are similar and remain unchanged for months at neutral pH. As previously observed, the PEG chains may have a protecting effect against the hydrolysis of the imine bonds, favouring the imine formation.⁷ On progressive addition of cationic molecular heads **3** to **A1–5** mixtures in water, the ¹H-NMR spectra are reminiscent with the formation of completely condensed frameworks (Fig. S1–S5 and Tables S2–S6†). The conversion of the aldehyde groups is total on the addition of 0.2 eq. of cationic head **3**. We noticed that, at low concentrations of **3** (0.4, 0.6, 0.8 eq.), insoluble aggregates are formed in aqueous solution. When the amount of bPEI is increased (1–3 eq.), the hydrophilic behaviour and thus the solubility of colloids in water also increase. The ¹H-NMR spectra of all combinations are consistent with the formation of completely condensed imine-networks. This is indicated by the analysis of chemical shifts of the imine and aromatic moieties, which shows for all cases similar and broad patterns of signals, reminiscent of exchanging dynamic networks in solution. Gel electrophoresis DNA binding experiments showed similar binding



Scheme 1 Schematic representation of the synthesis of DCFs combining 1,3,5-benzenetri-aldehyde cores **1** (red circle) with PEG **2** (green) in acetonitrile. Further treatment of this mixture with positively charged PEI **3**, heads (blue) in water generates DCFs. All the reactions have been performed for different molar ratios of components – see the text for details.

Table 1 Different molar ratios of **1** : **2** : **3** used for the synthesis of DCF1–6

DCF	1	2	3
1	1	1	1.5
2	1	1	2
3	1	1	3
4	3	2	1.5
5	3	2	2
6	3	2	3

behaviour for all studied combinations (Table S7, ESI†). At this point, we focused our next studies on a reduced series of DCF1–6 concerning two series of linear DCF1–3 and cross-linked DCF4–6 networks with different charge contents (Table 1).

X-ray photoelectron spectrometry – XPS experiments

The reactions between 1,3,5-benzenetri-aldehyde **1**, PEG **2**, and bPEI **3** building block precursors are also confirmed by using high resolution XPS spectra. Fig. S6 in ESI† describes the wide scan spectra of **1–3** and DCF1, **3** and **6**, respectively. A high

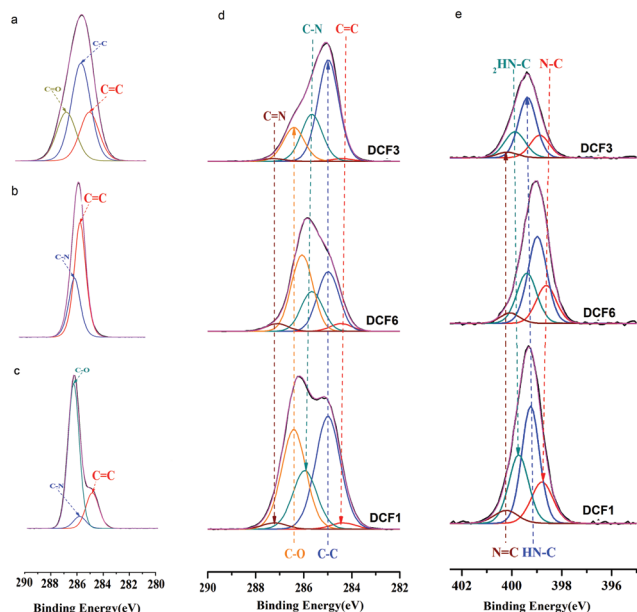


Fig. 1 Deconvoluted high resolution XPS spectra of C 1s peaks of (a) 1, (b) 2, (c) 3, (d) DCF1, 3, 6 and (e) N 1s peaks of DCF1, 3, 6.

resolution C 1s peak between 281.8 and 289.2 eV observed for the 1,3,5-benzenetrialdhyde 1 sample (Fig. 1a) was deconvoluted in three characteristic peaks at 284.4, 285 and 286.1 eV attributed to C=C, C-C/C-H, C=O bonds, respectively. The C 1s peak ranged between 282.8 eV and 287.1 eV observed for the PEG 2 sample (Fig. 1b) reveals three deconvoluted peaks corresponding to C-C/C-H at 285 eV, C-N at 286 eV and C-O at 286.5 eV, respectively. Finally, specific C 1s types of bindings have been observed for bPEI sample 3 with specific peaks for C-C/C-H and C-N bonds at 285 and 285.4 eV, respectively (Fig. 1c). The deconvoluted C 1s and N 1s spectra for DCF1, DCF3 and DCF6 are represented in Fig. 1d and e respectively. They are fitted with five and four peaks, attributed to C=C, C-C/C-H, C-N, C-O and C=N bonds at 284.4–284.5, 285.0, 285.7–286.0, 286.1–286.4 and 287.1–287.3 eV and to N-C at 398.6–398.9 eV, HN-C at 399–399.4 eV, NH₂-C at 399.5–399.9 eV and N=C at 400.1–400.2 eV, respectively. These data are in agreement with the total conversion of the aldehyde groups into imine groups, in perfect agreement with the results determined by ¹H-NMR. Elemental compositions calculated based on the wide scan XPS spectra of investigated precursors and DCFs are in agreement with the theoretically calculated ones (Tables S8 and S9, ESI†).

DNA polyplexes based on the DCF1, DCF3 and DCF6

Three types of polyplexes of DCF1, DCF3 and DCF6 were generated by mixing DCFs with linear dsDNA (salmon sperm DNA; ~200–300 base pairs) and a circular dsDNA (plasmid pCS2+MT-Luc; 5991 base pairs). All related studies were performed considering compositions precisely formulated between the carriers and the dsDNA, calculated as ratios between the molar

fraction N/P of nitrogen in the DCF conjugates and the molar content of phosphorus in the DNAs.

Morphological and dimensional behaviour of DNA/DCF polyplexes

To ensure prolonged circulation in blood vessels, the polyplex particle size should be compacted, roughly between 10 and 200 nm. Entities below 10 nm are quickly cleared through the kidney, while the ones above 200 nm are cleared by the reticulo-endothelial system.^{12d} For these reasons it was important to determine the size of particulate DNA polyplexes, generated by DCF-dsDNA association in aqueous solution. First, we investigated their solution behavior by Dynamic Light Scattering (DLS) (Fig. 2a). Our results show that DCFs have an average diameter of 3 nm, while DCF·salmon sperm dsDNA polyplexes

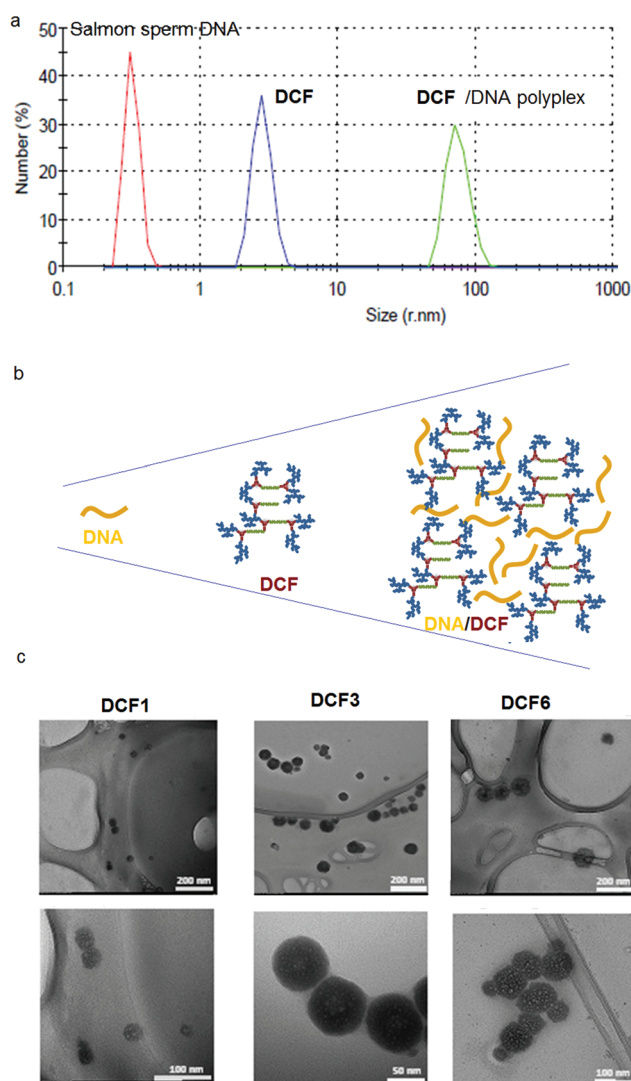


Fig. 2 (a) DLS measurements for dsDNA, DCF and dsDNA:DCF polyplex; (b) size of dsDNA, DCF and dsDNA:DCF polyplex and their proposed self-aggregation mechanism; (c) TEM micrographs for DCF1, 3, 6-pCS2+MT-Luc polyplexes at N/P = 10.

have an average diameter of 80 nm. This suggests that salmon sperm dsDNA with sub-nanometric dimensions is well packed by the DCF, leading to the formation of bigger aggregates, in which likely several DNA molecules fold and bind around several DCFs (Fig. 2b).

TEM imaging (Fig. 2c) showed the formation of spherical aggregates, whose sizes vary between 40 and 125 nm, depending on the 1 : 2 : 3 molar ratio; the aggregates display a narrow size distribution within each sample. The inside areas of the aggregates present different densities, perhaps due to a different packaging capacity of conjugates for DNA, determined by the availability of the positive charges of bPEI conjugates toward negative charges of DNA.

DNA binding ability of DCF1–6 polyplexes

The DNA binding ability of DCF1–6 polyplexes was investigated by agarose gel electrophoresis (Fig. 3). Salmon sperm dsDNA or plasmid pCS2+MT-Luc was complexed with DCF1–6, at different N/P ratios. In the case of the linear salmon sperm dsDNA, polyplex electrophoretic migration is completely blocked at an N/P ratio = 3. At this value, DLS and TEM analysis shows that packing between DNA and DCF1–6 takes place with the formation of aggregates in solution and in the solid state. These results also agree with previous reports, showing that nearly all DNA is packed by bPEI of 25 kDa for an N/P ratio = 3 and that transfection efficiency can be enhanced for higher N/P ratios.^{12c} We observed a significant difference between the ability of DCFs to condense salmon sperm dsDNA

versus the stiffer, higher molecular weight pCS2+MT-Luc plasmid DNA. Electrophoretic migration of plasmid DNA is completely blocked for N/P ratios above 5 in the case of DCF1–6. In this respect, a levelling effect is obvious in the case of N/P = 1 or 3 where DCF1–6 are less effective in binding plasmid DNA. Comparatively, for these N/P ratios, the best binding is observed for DCF3, suggesting a good balance between the linear geometry of the PEG backbone and the high content of bPEI, which is perhaps optimal for packaging and protection of plasmid DNA.

Transfection ability

We measured the transfection efficiency of DCF1, 3 and 6 polyplexes by assaying the uptake by HeLa cells of pCS2+MT-Luc plasmid, which drives expression of firefly luciferase. HeLa cells were treated with polyplexes formed by mixing a fixed quantity of pCS2+MT-Luc DNA plasmid (400 ng per well of a 96-well plate) with varying amounts of DCFs, followed by luciferase assays 48 hours later. As shown in Fig. 4, all tested polyplexes transfect HeLa cells to a level comparable with bPEI, or slightly better at N/P ≥ 100 .¹³

Cytotoxicity of DCF1–6 and DCF1–6 polyplexes

To assess toxicity of DCF1, 3, 6 polyplexes, we used an assay that measures mitochondrial reductase activity (MTS).¹⁴ Only cells with the uncompromised mitochondrial function reduce tetrazolium salt to formazan. Using this assay, we observed an increase in cell viability with decreasing N/P ratios; interestingly, a slight increase in cell proliferation relative to untreated controls was observed for N/P ratios of less than 150. We determined that cells treated with DCF1 and DCF6 and their polyplexes show the highest viability, while DCF3 and bPEI 800 show higher toxicity (Fig. 5). DCF1 and DCF6 with higher PEG

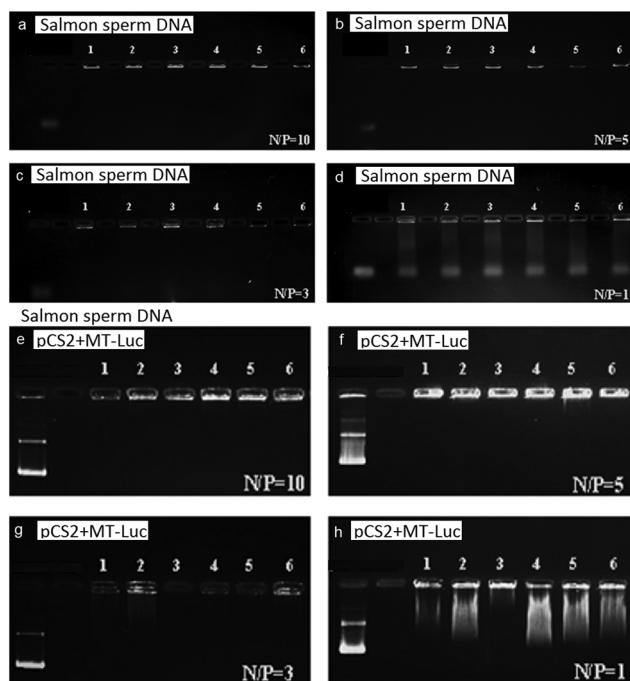


Fig. 3 Agarose gel retardation assays in the case of DCF1–6-salmon sperm dsDNA at (a) N/P = 10, (b) N/P = 5, (c) N/P = 3, (d) N/P = 1 ratios and DCF1–6-pCS2+MT-Luc polyplexes at (e) N/P = 10, (f) N/P = 5, (g) N/P = 3, (h) N/P = 1 ratios.

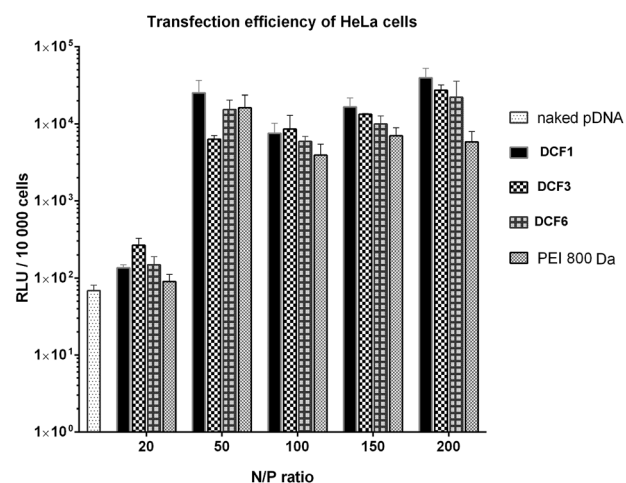


Fig. 4 Transfection efficiency at different N/P ratios measured at 48 hours. HeLa cells were treated with polyplexes made by combining pCS2+MT-Luc plasmid with polymers: DCF1, DCF3, DCF6 and PEI 800. Naked pDNA is presented as the reference. The results are given as relative light units per 10 000 cells.

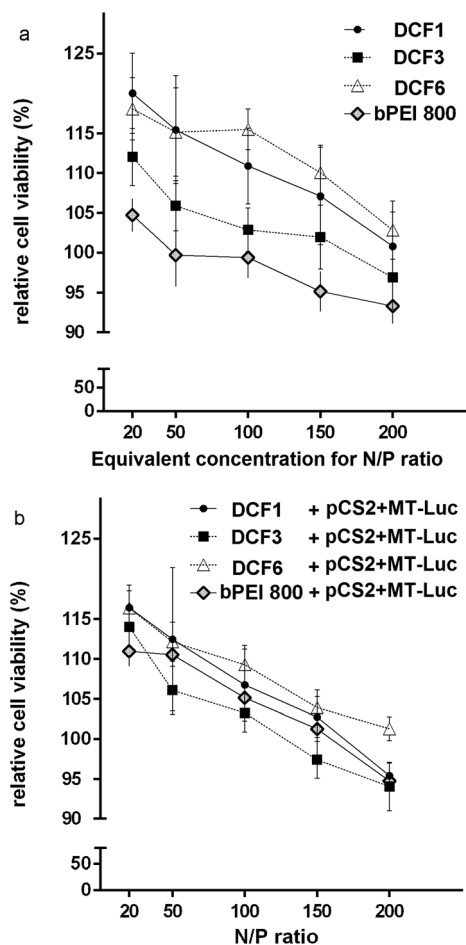


Fig. 5 Cytotoxicity profiles of (a) DCF1, 3, 6 and PEI and (b) their respective DCF1, 3, 6 (used at the same concentration with that employed to calculate N/P) and PEI-pCS2+MT-Luc polyplexes based on the MTS assay. The viability of cells grown in medium alone (control cells) was considered 100%.

content lead to increased cellular proliferation compared to DCF3 that incorporates a higher fraction of bPEI. DCF3 showing high DNA binding and transfection ability and having the highest bPEI concentration is associated with higher cytotoxicity. Our findings are in accord with the effect of PEG on cytotoxicity that has been described in previous studies.¹⁵

Conclusions

The present study describes the synthesis and characterization of a class of DNA nanovectors based on specific frameworks of components and connector centres, linked by reversible covalent bonds. The dynamic self-assembly of PEG components with bPEI cationic binding groups around the aromatic core connectors leads to adaptive spatial distributions in the presence of interacting DNA biotargets.

The DCF polyplexes reported here are able to act as gene nanovectors, by forming stable polyplexes with dsDNA.

Depending on the type and amount of associated DNA and on the molar ratio of bPEI/PEG, polyplexes have dimensions ranging between 40 and 125 nm. All tested vectors were capable of transfecting DNA into HeLa cells and demonstrated low cytotoxic levels; even at an N/P = 200 cell viability is over 90% relative to untreated control cells. We can conclude that the presence of the PEG component and a moderate amount of b-PEI in DCFs are both important in the construction of highly transfecting and cyto-friendly polyplexes. Perhaps an optimal balance between the linear geometry of the PEG backbone and the high content of bPEI favours optimal packaging and protection of DNA. Furthermore, cell viability was always above 90%, demonstrating that our vectors are well tolerated by cells.

Our findings provide novel insights into the development, *via* a simple synthetic strategy, of multivalent adaptive nanovectors carrying out several functionalities for optimal DNA binding, membrane penetration, DNA delivery and anti-opsonisation functions. We believe that the approach presented here has the potential to solve critical problems in DNA delivery to cells that stem from the enormous variability of both DNA targets and cell types to be transfected. Work is currently in progress to further develop such dynamic adaptive systems.

Experimental section

Materials

1,3,5-Benzenetricarboxaldehyde (97%) **1** was purchased from Manchester Organics. Poly(ethylene glycol)bis(3-aminopropyl) terminated (PEG, $M_n \sim 1500 \text{ g mol}^{-1}$) **2** and branched polyethyleneimine (bPEI, 800 Da) **3** were purchased from Sigma-Aldrich, and were used without further purification. Low molecular weight salmon sperm DNA was purchased from Fluka (St Louis, MO, USA).

Synthesis of A1

1,3,5-Benzenetricarboxaldehyde (0.3014 g, 1.8582 mmol) was dissolved in acetonitrile (40 ml) under magnetic stirring. To this mix was added PEG (2.7884 g, 1.8582 mmol) dissolved in acetonitrile (10 ml), and the reaction was stirred for 72 hours, at room temperature. The solvent was removed by rotary evaporation (40 °C, under vacuum), affording the product (2.8 g).

Synthesis of DCF1

A1 (0.030 g, containing 0.0202 mmol of **1**) was dissolved in water (1 ml). To this solution was added bPEI (0.024 g, 0.0303 mmol) dissolved in water (0.284 ml). The reaction was stirred for 12 hours on a vortex and then incubated at room temperature for 72 h.

NMR

Spectra were recorded on a Bruker instrument operated at 300 MHz. All samples were dissolved in D_2O and analyzed at room temperature. Chemical shifts were recorded in ppm.

X-ray photoelectron spectroscopy (XPS)

X-ray photoelectron spectra (XPS) were recorded with a Kratos Axis Nova instrument (Kratos Analytical, Manchester, UK), using Al K α radiation, with 20 mA current and 15 kV voltage (300 W). XPS survey spectra were recorded in the range of –10 to 1200 eV with a resolution of 1 eV and a pass energy of 160 eV. For all elements identified from survey spectra, high-resolution spectra were recorded using a pass energy of 20 eV and a step size of 0.1 eV. Data were analysed using Vision Processing software (Vision2 software, Version 2.2.10). The binding energy of the C 1s peak was normalized to 285 eV.

Particle size measurements

Particle size measurements were performed on a Nano Zetasizer (Malvern Instruments Ltd, UK) operating at 633 nm and recording the back scattered light at an angle of 173°. Measurements were done in a cuvette with a 10 mm path length. The sample temperature was allowed to equilibrate for 3 min before each measurement. The light scattering was recorded for 200 s with 10 replicate measurements.

TEM microscopy images

TEM microscopy images were obtained on a HT7700 Hitachi Transmission Electron Microscope. Samples were prepared by placing a drop of aqueous suspension of polyplexes on a carbon-coated copper grid, then allowing the solvent to evaporate at room temperature. The grids were imaged in high-resolution mode, under an operating potential of 100 kV. For each sample, the size of 500 aggregates was measured from TEM micrographs, using Image J software.

Preparation of plasmid DNA

Plasmid pCS2+MT-Luc which encodes for firefly luciferase (Harvard University, Boston) was propagated by molecular cloning in *E. coli* DH5 α , extracted and purified with an E.Z.N.A. Endo-free Plasmid Mini II kit (Omega Bio-Tek, Inc.).

Preparation of polyplexes

The polymer was dissolved in pure water (Millipore), after which an appropriate amount of DNA was added and the mix was vortexed for 10 s, followed by incubation for 30 minutes before use.

Gel retardation assay

Polyplexes were prepared with varying N/P ratios: 10, 5, 3 and 1. The polyplex solution (5 μ L polymer and 5 μ L salmon sperm DNA/1 μ L plasmid solutions) was mixed with 3 μ L TAE buffer, pH = 7.4 and 10 μ L sucrose solution. The samples were then loaded on a 1% agarose gel. Electrophoresis was carried out at 90 V for 60 minutes for salmon sperm DNA and 120 minutes for the plasmid. The gel was stained with ethidium bromide and was then imaged on a UV transilluminator.

Cell culture

Transfection of DNA by polyplexes was assayed in HeLa cells. HeLa cells (from CLS-Cell-Lines-Services-GmbH, Germany)

were grown in tissue culture flasks with alpha-MEM medium (Lonza) supplemented with 10% fetal bovine serum (FBS, Gibco) and a penicillin–streptomycin–amphotericin B mixture (Lonza).

Measuring *in vitro* transfection efficiency

HeLa cells were harvested by trypsinization, counted with a Countess Automated Cell Counter (Invitrogen), and seeded at a density of 10⁴ cells per well in 96 well white opaque culture microplates (PerkinElmer) with 100 μ L per well. Cells were transfected 24 hours later with 400 ng of pDNA per well, mixed with DCFs or bPEI (800 Da) at various N/P ratios. Both pDNA and polymers were separately diluted in 10 μ L alpha-MEM without FBS and antibiotic. These 2 solutions were then mixed, vortexed briefly and then incubated at room temperature. After one hour, the transfection mixture was added to cells without removing the medium. After 48 hours, transfection efficiency was evaluated with a Bright-Glo(TM) Luciferase Assay System kit (Promega) on an EnSight plate reader (Perkin-Elmer). Each experiment was performed in triplicate.

Cytotoxicity assay

Cytotoxicity was measured using the CellTiter 96® Aqueous One Solution Cell Proliferation Assay (Promega). HeLa cells were seeded at a density of 10⁴ cells per well in 96 well plates, in 100 μ L DMEM without phenol red (Lonza) supplemented with 10% FBS. The next day, cells were transfected with polyplexes as described above, after which the cells were grown for another 44 hours. At least 3 biological replicates were performed for each polyplex type and N/P ratio, and each experiment was repeated 3 times. After 44 hours, 20 μ L of CellTiter 96® Aqueous One Solution reagent were added to each well, and the plates were incubated for another 4 hours before reading the result. Absorbance at 490 nm was recorded with an EnSight plate reader (PerkinElmer).

Acknowledgements

This work was supported by a grant of the Romanian National Authority for Scientific Research, CNCS-UEFISCDI, project number PN-II-ID-PCCE-2011-2-0028.

Notes and references

- 1 M. Laird Forrest, G. E. Meister, J. T. Koerber and D. W. Pack, *Pharm. Res.*, 2004, **21**, 365.
- 2 Y. Wen, S. Pan, X. Luo, W. Zhang, Y. Shen and M. Feng, *J. Biomater. Sci., Polym. Ed.*, 2010, **21**, 1103.
- 3 J. H. Jeong, S. W. Kim and T. G. Park, *Prog. Polym. Sci.*, 2007, **32**, 1239.
- 4 (a) S. Bhattacharya and A. Bajaj, *Chem. Commun.*, 2009, 4632; (b) F. Heitz, M. C. Morris and G. Divita, *Br. J. Pharmacol.*, 2009, **157**, 195; (c) V. Bagnacani, V. Franceschi, M. Bassi, M. Lomazzi, G. Donofrio, F. Sansone, A. Casnati and

- R. Ungaro, *Nat. Commun.*, 2013, **4**, 1721; (d) M. Nishihara, F. Perret, T. Takeuchi, S. Futaki, A. N. Lazar, A. W. Coleman, N. Sakai and S. Matile, *Org. Biomol. Chem.*, 2005, **3**, 1659; (e) A. Montellano, T. Da Ros, A. Bianco and M. Prato, *Nanoscale*, 2011, **3**, 4035; (f) D. Sigwalt, M. Holler, J. Iehl, J.-F. Nierengarten, M. Nothisen, E. Morin and J.-S. Remy, *Chem. Commun.*, 2011, **47**, 4640; (g) M. Raouane, D. Desmaele, M. Gilbert-Sirieix, C. Gueutin, F. Zouhiri, C. Bourgaux, E. Lepeltier, R. Gref, R. B. Salah, G. Clayman, L. Massaad-Massade and P. Couvreur, *J. Med. Chem.*, 2011, **54**, 4067; (h) C. O. Mellet, J. M. Benito and J. M. Garcia Fernandez, *Chem. – Eur. J.*, 2010, **16**, 6728.
- 5 S. Mao, M. Neu, O. Germershaus, O. Merkel, J. Sitterberg, U. Bakowsky and T. Kissel, *Bioconjugate Chem.*, 2006, **17**, 1209.
- 6 C. Gehin, J. Montenegro, E.-K. Bang, A. Cajaraville, S. Takayama, H. Hirose, S. Futaki, S. Matile and H. Riezman, *J. Am. Chem. Soc.*, 2013, **135**, 9295.
- 7 R. Catana, M. Barboiu, I. A. Moleavin, L. Clima, A. Rotaru, E. L. Ursu and M. Pinteala, *Chem. Commun.*, 2015, **51**, 1991.
- 8 (a) C. Bouillon, D. Paolantoni, J. Rote, Y. Bassin, L. W. Peterson, P. Dumy and S. Ulrich, *Chem. – Eur. J.*, 2014, **20**, 14705; (b) S. Duan, W. Yuan, F. Wu and T. Jin, *Angew. Chem., Int. Ed.*, 2012, **51**(32), 7938.
- 9 (a) W. G. Skene and J.-M. Lehn, *Proc. Natl. Acad. Sci. U. S. A.*, 2002, **99**, 8270; (b) J.-M. Lehn, *Prog. Polym. Sci.*, 2005, **30**, 814; (c) L. Marin, B. Simionescu and M. Barboiu, *Chem. Commun.*, 2012, **48**, 8778; (d) L. Marin, S. Moraru, M.-C. Popescu, A. Nicolescu, C. Zgardan, B. C. Simionescu and M. Barboiu, *Chem. – Eur. J.*, 2014, **20**, 4814.
- 10 (a) G. Nasr, A. Gilles, T. Macron, C. Charmette, J. Sanchez and M. Barboiu, *Isr. J. Chem.*, 2013, **53**, 97; (b) G. Nasr, T. Macron, A. Gilles, C. Charmette, J. Sanchez and M. Barboiu, *Chem. Commun.*, 2012, **48**, 11546; (c) G. Nasr, T. Macron, A. Gilles, Z. Mouline and M. Barboiu, *Chem. Commun.*, 2012, **48**, 6827; (d) G. Nasr, T. Macron, A. Gilles, E. Petit and M. Barboiu, *Chem. Commun.*, 2012, **48**, 7398–7400.
- 11 T. G. Park, J. H. Jeong and S. W. Kim, *Adv. Drug Delivery*, 2006, **58**, 467.
- 12 (a) H. Petersen, P. M. Fechner, A. L. Martin, K. Kunath, S. Stolnik, C. J. Roberts, D. Fischer, M. C. Davies and T. Kissel, *Bioconjugate Chem.*, 2002, **13**, 845; (b) M. Ogris, S. Brunner, S. Schuller, R. Kircheis and E. Wagner, *Gene Ther.*, 1999, **6**, 595; (c) Z. Dai, T. Gjetting, M. A. Matthebjerg, C. Wu and T. L. Andersen, *Biomaterials*, 2011, **32**, 8626; (d) R. A. Petros and J. M. DeSimone, *Nat. Rev. Drug Discovery*, 2010, **9**, 615.
- 13 C. Y. M. Hsu and H. Uludag, *Nat. Protocols*, 2012, **7**, 935.
- 14 (a) J. A. Barltrop, T. C. Owen, A. H. Cory and J. G. Cory, *Bioorg. Med. Chem. Lett.*, 1991, **1**, 611; (b) J. C. Stockert, A. Blázquez-Castro, M. Cañete, R. W. Horobin and Á. Villanueva, *Acta Histochem.*, 2012, **114**, 785–796.
- 15 (a) H. Lv, S. Zhang, B. Wang, S. Cui and J. Yan, *J. Controlled Release*, 2006, **114**, 100; (b) H. Lee, J. H. Jeong and T. G. Park, *J. Controlled Release*, 2002, **79**, 283.